



**Information Science** — *Efficient Representation in Spaces of Plane Curves*, by KATHRYN LEONARD, communicated on 14 November 2008.

**ABSTRACT.** — This paper evaluates the Blum medial axis representation of embeddings of  $S^1$  into  $\mathbb{R}^2$  from the perspective of efficiency, using a  $C^1$ -type metric. For compact classes of curves with Lipschitz tangent angle, we compute the  $\varepsilon$ -entropy and compare that efficiency benchmark with uniform approximation using the Blum medial axis. In the compact setting, the boundary curve is more efficient. For noncompact classes of embeddings, we establish a geometric criterion for when the medial axis will be more efficient in an adaptive approximation.

**KEY WORDS:** Shape approximation; epsilon-entropy; medial axis.

**MATHEMATICS SUBJECT CLASSIFICATION (2000):** 41; 58

## 1. INTRODUCTION

The quest for sparse representation in linear spaces, spearheaded by the  $x$ -let community, suggests the following moral: The optimal basis for a function class is the one that most efficiently captures the salient structures of that class. In this paper, we apply the same moral in a nonlinear setting. Spaces of plane curves, the simplest examples of nonlinear spaces, have recently attracted substantial research activity prompted by questions of shape recognition and analysis arising from computer vision [2, 10, 17, 19, 23]. We contribute to that growing body of work by applying ideas of sparse representation to the approximation of curves. In particular, we compare representing an embedded, closed curve with Lipschitz tangent angle using its boundary with representing it using its medial axis pair, for both compact and noncompact classes of closed plane curves. Just as for linear spaces, we find striking differences between results for compact and noncompact settings.

The Blum medial axis pair is a subset of the symmetry set of an embedded, closed curve. It can be viewed as the skeleton and ribs of the enclosed region, where the skeleton is a deformation retract of the boundary curve, and the rib at a point on the skeleton is the distance that point has traveled. Perhaps its mathematical relevance is best suggested by the number of mathematical perspectives reformulating its definition. It can be defined variously as: the locus of centers of maximal circles contained within the boundary together with the radii [3], the shock set formed by evolving the boundary under pure reaction together with time to shock formation [1, 22], the zero set of a distance function [15], or a Whitney stratified set with a vector field satisfying certain properties [5, 9]. In addition, it has close links to certain equivalence classes of quasisymmetric homeomorphisms of  $S^1$  [7].

We begin by offering necessary background material in Section 2. Our result in Proposition 5 provides the foundation for our later work in noncompact classes of curves (Section 5). We consider uniform approximation and  $\varepsilon$ -entropy in Section 3, constructing approximations that show the boundary curve to be a near-optimal representation for curves in the compact case. Section 4 constructs a covering for compact classes using the medial axis representation which shows the medial axis to be sub-optimal. Section 5 addresses efficiency in noncompact classes of curves, determining a geometric criterion for when the medial axis will be more efficient than the boundary.

In the course of our investigation, we obtain near-tight estimates of  $\varepsilon$ -entropy for our compact classes of curves. These are among the first such results for classes of geometric objects. Bronshtein computed  $\varepsilon$ -entropy for classes of convex sets [4], while Dudley, who found the appropriate order for  $\varepsilon$ -entropy for classes of interiors of closed plane curves using the Hausdorff metric, made no attempt to find the constant [6]. Note that some of the results presented here are the mathematical formulations of results published in [13].

## 2. BACKGROUND

### 2.1. Spaces of Plane Curves

Consider the space  $\mathcal{C}$  of  $C^1$  curves  $\gamma(s) : [0, L_\gamma] \rightarrow \mathbb{R}^2$  for  $L_\gamma \geq 0$  satisfying:

- (a)  $\|\gamma'(s)\| \equiv 1$
- (b)  $\gamma(0) = 0$  and  $\gamma'(0) = (1, 0)$ .

Within  $\mathcal{C}$  lie the closed curves,  $\mathcal{I}$ , immersions of  $S^1$  into  $\mathbb{R}^2$  (and also the embeddings  $\mathcal{E} \subset \mathcal{I}$ ).

We introduce a  $C^1$ -type metric on  $\mathcal{C}$ , with  $\lambda$  a dimension-normalizing constant. Given  $\gamma_1(s_1), \gamma_2(s_2) \in \mathcal{C}$ ,

$$\rho(\gamma_1, \gamma_2) = \sup_{i,j=1,2} \left\{ \sup_{\substack{s_j \\ j \neq i}} \inf_{s_i} \left( \frac{1}{\lambda} |\gamma_i(s_i) - \gamma_j(s_j)| + |\theta_i(s_i) - \theta_j(s_j)| \right) \right\},$$

where  $\theta_i(s_i)$  is the tangent angle to  $\gamma_i(s_i)$ .

Denote by  $\mathcal{C}_K^L \subset \mathcal{C}$  ( $\mathcal{I}_K^L \subset \mathcal{I}$ ,  $\mathcal{E}_K^L \subset \mathcal{E}$ ) those curves of length at most  $L$  satisfying  $|\theta(s) - \theta(t)| \leq K|s - t|$ . Identifying any sequence of curves  $\{\gamma_i\} \subset \mathcal{C}_K^L$  with the sequence of the tangent angles and lengths  $\{(\theta_i, L_i)\}$  for those curves, one may generate a convergent subsequence of  $\{\gamma_i\}$ , thereby showing that  $\mathcal{C}_K^L$  is compact in the metric  $\rho$ . As  $\mathcal{I}_K^L$  is a closed subset of  $\mathcal{C}_K^L$ , it too is compact. Note that for these compact spaces, one should ensure  $\lambda > 1/K$  in the definition of  $\rho$ .

While this paper presents theorems about  $\mathcal{C}$  and  $\mathcal{I}$ , its heart belongs to  $\mathcal{E}$ . An embedded closed curve can be represented in multiple ways (boundary curve, interior region, curvature function), but we focus on Blum's medial axis representation.

## 2.2. Blum's Medial Axis Pair

Intuitively, Blum's medial axis pair consists of a skeleton of curves  $\mathbf{m}$ , and a radius function  $r$  encoding the lengths of the ribs along the skeleton.

**DEFINITION.** *The medial axis pair  $(\mathbf{m}, r)$  consists of the closure  $\mathbf{m}$  of the locus of centers of circles that are bitangent to the boundary curve and whose radii, encoded in  $r$ , equal the minimum distances from the boundary curve to the centers.*

Generically, a  $C^p$  boundary curve will produce a skeleton  $\mathbf{m}$  consisting of  $C^p$  branches and a  $C^p$  radius function along each branch. These branches (generically) meet at the center of tritangent circle, so branches meet in threes [8, 14]. We will denote a branch by  $m(v)$ , where  $v$  is the arclength parameter on that branch. In addition, we point out that moving along a medial branch  $m(v)$  following its orientation sweeps out two portions of the boundary,  $\gamma_+(v)$  to the left of the medial branch and  $\gamma_-(v)$  to the right. We adopt the convention that  $\gamma_-$  is oriented with the orientation of the boundary curve, and  $\gamma_+$  is oriented opposite. In general, we will use subscripts  $\pm$  to refer to quantities associated to  $\gamma_\pm$  and subscript  $m$  to refer to quantities associated to  $m$ .

Explicit formulas relate the boundary curve to the medial axis pair:

$$(1) \quad \gamma_\pm(v) = (m + rr'T_m \mp r\sqrt{1 - r'^2}N_m)(v),$$

and vice versa:

$$r(s) = -\frac{(\gamma_+ - \gamma_-) \cdot (N_+ - N_-)}{(N_+ - N_-) \cdot (N_+ - N_-)},$$

$$m(s) = \gamma_\pm(s)r(s)N_\pm.$$

In addition, the geometry of the boundary is closely related to the geometry of the medial axis. As we see from the definitions, the radial vector from an axis point to an associated boundary point is orthogonal to the boundary at that point. Denote by  $\phi$  the angle between the tangent vector to  $m(v)$  and the outward pointing normal vector to  $\gamma_\pm$ , and by  $\theta_m(v)$  the tangent angle to  $m(v)$ . Refer to Figure 1. We immediately see that:

$$\theta_\pm = \theta_m \pm \phi + \frac{\pi}{2}.$$

Straightforward arguments show that:

$$(2) \quad r'(v) = \cos \phi,$$

$$(3) \quad \pm \kappa_m = \pm \frac{1}{2} \sin\left(\frac{\theta_+ - \theta_-}{2}\right) \left(\frac{\kappa_-}{1 - r\kappa_-} - \frac{\kappa_+}{1 - r\kappa_+}\right),$$

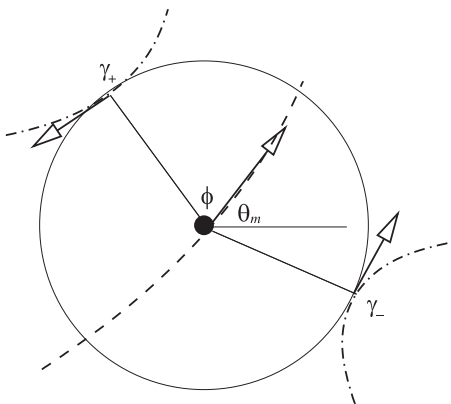


Figure 1. Relating the geometry of the medial axis to the geometry of the boundary curves  $\gamma_{\pm}$ .

$$(4) \quad \phi'(v) = -\frac{1}{2} \sin\left(\frac{\theta_+ - \theta_-}{2}\right) \left(\frac{\kappa_-}{1 - r\kappa_-} + \frac{\kappa_+}{1 - r\kappa_+}\right)$$

$$(5) \quad \frac{ds_{\pm}}{dv} = \frac{\mp \sqrt{1 - r'^2}}{1 - r\kappa_{\pm}}.$$

See [8, 14] for more details and further exploration of geometric relationships. We end by relating the number of branches in  $\mathbf{m}$  to the number of maxima of curvature for  $\gamma$ .

**LEMMA 1.** *Let  $\Omega$  be a bounded, simply connected region of the plane, and  $(\mathbf{m}, r)$  the medial axis pair for a generic, twice-differentiable closed, simple curve  $\gamma \subset \Omega$ . Then if  $\gamma$  has  $N$  local maxima of curvature, the number of branches in  $\mathbf{m}$  is at most  $2N - 3$ .*

**PROOF.** The medial axis of a generic curve consists of three types of points: points where the medial circle osculates at the endpoint of an axis branch, tritangent points where three medial branches come together, and bitangent points in the interior of a medial branch [8].

If the medial circle osculates at the endpoint of a branch,  $\gamma$  must have a local maximum of curvature at the point of osculation. On the other hand, every local maximum of curvature does not necessarily correspond to an osculating medial circle. Therefore, the number of endpoint branches is at most  $N$ .

Because  $\gamma$  is a simple, closed,  $C^2$  curve,  $\mathbf{m}$  is connected. As the deformation retract of the boundary of a contractible space, it is also contractible. Therefore, the graph of  $\mathbf{m}$  is a tree, where edges correspond to bitangent circles and vertices correspond to tritangent circles. Since vertices will only occur at tritangent points, a simple counting argument gives that the number of vertices for the medial graph with  $k$  endpoints is  $k - 2$ , which gives the number of edges as  $2k - 3$ . Hence the number of branches in  $\mathbf{m}$  is at most  $2N - 3$ .  $\square$

2.3. Functions and  $\varepsilon$ -entropy

An  $\varepsilon$ -cover for a subset  $X$  of a metric space  $(M, \rho)$  is a system of sets  $\{U_\alpha\}$  so that  $X \subseteq \bigcup_\alpha U_\alpha$  with the diameter of  $U_\alpha$  less than  $2\varepsilon$  for any  $\alpha$ . For totally bounded spaces, the number of elements in any reasonable  $\varepsilon$ -cover will be finite. Optimality of an particular  $\varepsilon$ -cover can be measured by comparing it to the benchmark given by the  $\varepsilon$ -entropy.

**DEFINITION.** *If  $N_\varepsilon$  is the cardinality of a minimal  $\varepsilon$ -cover on  $X$ , then the  $\varepsilon$ -entropy  $\mathcal{H}_\varepsilon(X, \rho) = \log_2 N_\varepsilon$ .*

When  $X$  has finite dimension, the exponent captured by the  $\varepsilon$ -entropy will be finite and will be a function of the dimension. When  $X$  has infinite dimension, the exponent will be a function of  $\varepsilon$ . Two totally bounded spaces with the same  $\varepsilon$ -entropy can be viewed as being the same “size.”

Classically,  $\varepsilon$ -entropy results are obtained by constructing an  $\varepsilon$ -cover for  $X$  with no more than  $K_\varepsilon$  elements, and a  $2\varepsilon$ -separated set (a collection  $\{x_i\} \subset X$  where  $\rho(x_i, x_j) \geq 2\varepsilon$  for  $i \neq j$ ) with at least  $L_\varepsilon$  elements, and showing that  $\lim_{\varepsilon \rightarrow \infty} \log K_\varepsilon / \log L_\varepsilon = 1$ , or at worst a non-zero constant.

The result we will use most is the following, due to Kolmogorov and Tikhomirov [11].

**THEOREM 2.** *For a fixed  $C > 0$ , let  $F$  be the collection of functions  $f : [a, b] \rightarrow \mathbb{R}$  satisfying  $|f(x) - f(y)| \leq C|x - y|$  and  $f(a) = c_0$ . Then:*

$$\mathcal{H}(F, L^\infty) = \begin{cases} \frac{|b-a|C}{\varepsilon} - 1 & \frac{|b-a|C}{\varepsilon} \in \mathbb{Z}^+ \\ \left\lceil \frac{|b-a|C}{\varepsilon} \right\rceil & \text{else.} \end{cases}$$

The proof follows the classical methodology. For the upper bound, construct an  $\varepsilon$ -covering via piecewise linear bounds to “corridors” with slopes  $\pm C$ , where the sign can change at  $x$ -values spaced at intervals of width less than  $\varepsilon/C$  (Figure 2). For the lower bound, construct a  $2\varepsilon$ -separated set via piecewise linear functions with slopes  $\pm C$  where the sign can change at  $x$ -values spaced at least  $\varepsilon/C$  apart. Counting the numbers  $K_\varepsilon$  and  $L_\varepsilon$  gives the result.

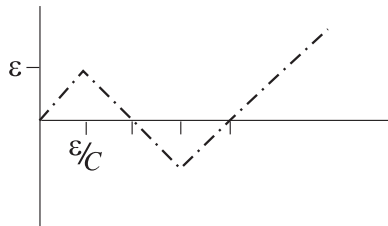


Figure 2. One piecewise linear function with slope  $\pm C$  providing an upper edge to a corridor of width  $2\varepsilon$ .

Modifying the class of Lipschitz functions above to include functions with  $|f(a)| \leq B$  gives an easy corollary [11]:

**COROLLARY 3.** *For fixed  $B, C > 0$ , let  $\tilde{\mathcal{F}}$  be the collection of functions  $f : [a, b] \rightarrow \mathbb{R}$  satisfying  $|f(x) - f(y)| \leq C|x - y|$  and  $|f(a)| \leq B$ . Then:*

$$\mathcal{H}(\tilde{\mathcal{F}}, L^\infty) = \left\lceil \frac{|b - a|C}{\varepsilon} \right\rceil + \left\lceil \log \frac{B}{\varepsilon} \right\rceil + O(1).$$

If instead of the  $L^\infty$  metric on Lipschitz functions, we use the  $C^1$  metric

$$\rho_1 = \sup_{x \in [a, b]} \left( \frac{1}{\lambda} |f(x) - g(x)| + |f'(x) - g'(x)| \right)$$

on functions with Lipschitz derivatives, we find that the leading order term in the cardinality of the covering comes from covering the derivative functions.

**THEOREM 4.** *For fixed  $C > 0$ , let  $G$  be the collection of functions  $f : [a, b] \rightarrow \mathbb{R}$  satisfying  $|f(x) - f(y)| \leq C|x - y|$  and  $f(a) = c_0, f'(a) = c_1$ . Then:*

$$\mathcal{H}_\varepsilon(G, \rho_1) \sim \left\lceil \frac{|b - a|C}{\varepsilon} \right\rceil.$$

**PROOF.** Let  $F$  be as in Theorem 2. This is the class of derivatives for functions in  $G$ . Given  $\varepsilon > 0$ , choose  $\delta_1$  to satisfy  $\varepsilon = \delta_1 + \delta_1^{3/2}/\lambda$  and construct a  $\delta_1$ -cover of  $(F, L^\infty)$  as described above, denoting the centers of the  $\delta_1$ -balls by  $\{f_i\}$ . This covering induces a coarse covering of  $(G, \rho_1)$  by taking primitives of functions in a given  $\delta_1$ -ball.

We now refine the induced covering. For  $\xi = 3/2$ , partition  $[a, b]$  into sub-intervals  $I_k = [x_{k-1}, x_k]$  of width at most  $\Delta = \delta_1^{\xi-1}/2$ . Refine an induced  $\delta_1$ -ball with center  $g_i(x) = \int_a^x f_i$  using a cover in which new centers  $\{g_{ij}\}$  are piecewise differentiable with derivative  $g'_{ij}(x) = f_i(x)$  for  $x \neq x_k$ , and with discontinuities at  $x = x_k$  for each  $k$  where  $g_{ij}$  “jumps” by  $\pm \delta_1^\xi/2$  to correct for location. See Figure 3.

Assign a function  $g$  in the original  $\delta_1$ -ball to a new ball by selecting the center so that  $g_{ij} = \arg \min_j |g(x_k) - g_{ij}(x_k)|$  for each  $k$ . By construction,  $f(a) = g_{ij}(a)$ . Assume  $|g(x_{k-1}) - g_{ij}(x_{k-1})| \leq \frac{\delta_1^\xi}{2}$  for some  $k$ . Then, for  $x \in I_k$ :

$$\begin{aligned} |g(x) - g_{ij}(x)| &\leq \int_{I_k} |g'(t) - g'_{ij}(t)| dt + \frac{\delta_1^\xi}{2} \\ &\leq \delta_1 \Delta + \frac{\delta_1^\xi}{2} \\ &= \delta_1^\xi. \end{aligned}$$

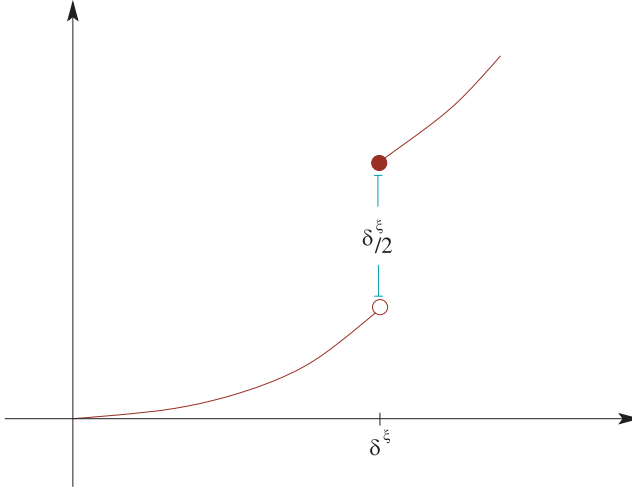


Figure 3. Jumps to correct the location of approximating functions  $g_{ij}$  [13].

This covering is therefore a  $(\delta_1 + \delta_1^\xi/\lambda)$ -cover (an  $\varepsilon$ -cover) for  $(G, \rho_1)$  with  $K_{\delta_1} = 2^{\lfloor b-a|C/\delta_1 \rfloor + \lfloor 2|b-a/\delta_1^{\xi-1} \rfloor}$ .

For the lower bound, choose  $\delta_2$  so that  $\varepsilon = \delta_2 + \delta_2^\xi/(2C\lambda)$ . Construct a  $2\delta_2$  separated set in  $\{f_i\} \subset (F, L^\infty)$  as described for Theorem 2. Then the collection of primitives  $\{g_i(x) = \int_a^x f_i\}$  satisfies:

1. For each  $i \neq j$  there exists  $x_{ij}$  so that  $|g'_i(x_{ij}) - g'_j(x_{ij})| \geq 2\delta_2$ .
2.  $|g_i(x_{ij}) - g_j(x_{ij})| \geq \int_a^{\delta_2/C} 2Ct dt = \delta_2^2/C$ ,

and so is a  $(\delta_2 + \delta_2^\xi/(2C\lambda))$ -separated ( $\varepsilon$ -separated) in  $(G, \rho)$  with  $L_{\delta_2} = 2^{\lfloor b-a|C/\delta_2 \rfloor}$  elements.

Finally, we observe that;

$$\lim_{\varepsilon \rightarrow 0} \frac{\log L_{2\delta_2}}{\frac{|b-a|C}{\varepsilon}} = \lim_{\varepsilon \rightarrow 0} \frac{\log K_{\delta_1}}{\frac{|b-a|C}{\varepsilon}} = 1,$$

thereby proving the theorem. □

### 2.4. Adaptive Encoding

Enumerating the balls in an  $\varepsilon$ -covering for a class gives an  $\varepsilon$ -encoding for that class, where the encoding of an element consists of describing the  $\varepsilon$ -ball to which it belongs. From that perspective, the  $\varepsilon$ -entropy provides a tight lower bound for

the codelength of a uniform encoding of any totally bounded class. Applying a similar perspective to unbounded spaces introduces the idea of adaptive encoding. Certainly, any uniform encoding of an unbounded space will give infinite codelengths. A first stab at finite codelengths might be to exhaust the space by encoding nested totally bounded subspaces. It turns out we can do better than that. The following proposition offers an adaptive encoding of a Lipschitz function on  $[a, b]$ , the parallel of Theorem 2 for unbounded classes of Lipschitz functions.

**PROPOSITION 5.** *For every  $\varepsilon > 0$ , there exists a countable codebook  $F_\varepsilon = \{f_1, f_2, \dots\}$ , depending only on  $\varepsilon$ , with the following property. For every Lipschitz function  $g$  defined on  $[a, b]$  so that  $f(a) = 0$  and  $f'(x)$  is continuous a.e., there are constants  $C(f, \delta)$  such that for all  $\delta$ , there is a codeword  $f_n \in F_\varepsilon$  such that  $\|f - f_n\|_\infty \leq \varepsilon$  and  $f_n$  has description length:*

$$L(f_n) \leq \left\lceil \frac{\int |f'| + \delta}{\varepsilon} \right\rceil + C(f, \delta).$$

**PROOF.** Because  $f'$  is Riemann integrable, there exists for any  $\delta > 0$  a rational step function  $g$  with steps at a finite number of rational points  $\{x'_k\}$  so that  $|f'| \leq g$  and  $\int g \leq \int |f'| + \delta$ . In other words, on each subinterval  $I_j = [x_j, x_{j+1}]$ ,  $g$  is constant and  $f$  is Lipschitz with constant  $g(x_j)$ . To relate this to Theorem 2, notice that  $g \equiv C$  gives that result.

Then, within each  $I_j$ , proceed as in the Kolmogorov result, selecting points spaced no more than  $\varepsilon/g(x_j)$  apart. There will be at most  $\left\lceil \frac{g(x'_j)|I_j|}{\varepsilon} \right\rceil + 1 = \left\lceil \frac{\int_{I_j} g(x)}{\varepsilon} \right\rceil + 1$  such points in  $I_j$ . Taking piecewise linear functions with slope  $\pm g(x_j)$  on  $I_j$  as boundaries of corridors of width  $2\varepsilon$ , we denote the center of such a corridor by  $f_n$ . That center  $f_n$  will be the  $\varepsilon$ -approximation to  $f$ .

To encode  $f_n$  requires encoding only  $g$  and the signs for the slope changes within each  $I_j$ . As  $g$  has a finite number of rational values, its encoding is finite and independent of  $\varepsilon$ . Describing the sign changes requires a single bit at each of the possible change locations, which requires at most:

$$\sum_j \left( \left\lceil \frac{\int_{I_j} g}{\varepsilon} \right\rceil + 1 \right) + m \leq \left\lceil \frac{\int_{[a,b]} g}{\varepsilon} \right\rceil + 2m$$

bits. Then, absorbing  $2m$  into  $C(f, \delta)$ , the total number of bits required to describe  $f_n$  is:

$$L(f_n) \leq \frac{\int g}{\varepsilon} + C(f, \delta) \leq \frac{\int |f'| + \delta}{\varepsilon} + C(f, \delta),$$

as claimed. □

3. CURVES AND  $\varepsilon$ -ENTROPY

In this section, we derive the analogue of Theorem 4 for curves, presented below. Recall that  $\mathcal{C}_K^L$  and  $I_K^L$  are collections of curves with finite arclength whose tangent angle functions are Lipschitz, and that the metric  $\rho$  is the geometric equivalent of a  $C^1$ -metric.

To find an upper bound for an  $\varepsilon$ -cover for  $\mathcal{C}_K^L$  (and therefore  $\mathcal{I}_K^L$ ), we apply Theorem 2 to the associated class of tangent angle functions, again taking  $\delta_1$  to satisfy  $\varepsilon = \delta_1 + \delta_1^\xi$  for  $\xi = 3/2$ . To construct the covering, we refine the resulting covering of tangent angle functions as before, creating centers of jumps which are piecewise Lipschitz curves. Now instead of two directions for jumps (up or down) as in the function case, we require three evenly spaced directions. See Figure 4. The additional cost for this refinement to guarantee  $(\frac{\sqrt{\delta^3}}{\lambda} + \delta)$ -approximation of curves, given a  $\delta_1$ -cover in  $L^\infty$  for the tangent angle functions, turns out to be at most  $2^{\log 3 \lceil 4L/\sqrt{\delta_1^3} \rceil}$  additional elements per ball.

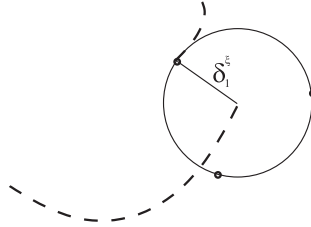


Figure 4. Possible locations for jumps of distance  $\delta_1^\xi$  in boundary approximation to correct for location.

**PROPOSITION 6.** *There exists a  $(\delta + \frac{\sqrt{\delta^3}}{\lambda})$ -cover for  $(\mathcal{C}_K^L, \rho)$  with no more than:*

$$\left\lceil \frac{4L}{\sqrt{\delta^3}} \right\rceil 2^{\lceil KL/\delta \rceil + \log 3 \lceil 4L/\sqrt{\delta} \rceil}$$

*elements.*

**PROOF.** To construct the cover, partition the interval  $[0, L]$  of possible arclength into subintervals of width  $\frac{\sqrt{\delta_1^3}}{4}$ , giving  $\left\lceil \frac{4L}{\sqrt{\delta_1^3}} \right\rceil$  subintervals. Let  $l_{\delta_1}$  be the right endpoint of any such subinterval. We will parameterize  $\gamma$  of length  $l \in \left( l_{\delta_1} - \frac{\sqrt{\delta_1^3}}{4}, l_{\delta_1} \right]$  by  $s \in [0, l_{\delta_1}]$  so that  $\gamma(0) = 0$ ,  $\theta(0) = 0$  and  $\frac{d\gamma}{ds} = \frac{l}{l_{\delta_1}}$ .

For all curves with lengths in a particular subinterval,  $|d\theta/ds| \leq \frac{l}{l_{\delta_1}} K \leq K$ , and so we may apply Theorem 2 to obtain an  $L^\infty$   $\delta_1$ -cover for the angle functions with at most  $2^{\lceil KL/\delta_1 \rceil}$  elements. Each of the resulting balls can be refined with no more than  $2^{\log 3 \lceil 4L/\sqrt{\delta_1^3} \rceil}$  additional elements. Applying this process within each length subinterval gives the result.  $\square$

The lower bound for  $\mathcal{C}_K^L$  requires more delicacy than the lower bound for functions in Theorem 4. Because the closest point to  $\gamma(s_0)$  on  $\tilde{\gamma}(s)$  might be for a large value of  $|s - s_0|$ , we must guard against curves bending back around to violate the required  $2\varepsilon$  distance.  $\mathcal{F}_K^L$  offers the additional difficulty that the curves must be closed. We address the problem for  $\mathcal{C}_K^L$  by constructing curves that are also functions (and therefore move primarily in a horizontal direction), but lose tightness of the lower bound for  $\mathcal{F}_K^L$  by requiring that the curves be closed.

**PROPOSITION 7.** *There exists a  $2\varepsilon$ -separated set for  $(\mathcal{C}_K^L, \rho)$  with  $\mathcal{M}_{2\varepsilon}$  elements, where  $\mathcal{M}_{2\varepsilon} \succeq 2^{\lfloor KL/\varepsilon \rfloor}$ .*

**PROOF.** Given  $\varepsilon > 0$ , choose  $\delta_2$  to satisfy  $\varepsilon = \frac{\delta_2}{1 + \frac{K^2\delta_2}{4}}$ . For  $L' = \frac{L}{\sqrt{1 + \frac{K^2\delta_2}{4}}}$ , divide

the interval  $[0, L']$  into subintervals  $I_k = [a_k, a_{k+1}]$  of width  $\sqrt{\delta_2}$ .

We claim that within the class of functions defined on  $I_k$  satisfying  $\int_{I_k} f_{ik} = 0$ ,  $f_{ik}(a_k) = f_{ik}(a_{k+1}) = 0$ , and  $|f(x) - f(y)| \leq K|x - y|$ , there is an  $L^\infty$   $2\delta_2$ -separated set  $\{f_{ik}\}$  with  $M_{2\delta_2}^k$  elements, where  $M_{2\delta_2}^k \preceq 2^{K|I_k|/\delta_2}$ . Note that by construction  $\|f_{ik}\|_\infty \leq \frac{K\sqrt{\delta_2}}{2}$ . We postpone proof of this claim. Given this  $2\delta_2$ -separated set, we will construct a collection of functions that are  $2\varepsilon$ -separated as curves. Taking primitives results in a collection of functions (now viewed as curves)  $\{g_{ik}\}$  with curvature bounded by  $K$  and tangent angle functions  $\{\theta_{ik}\} = \{\arctan f_{ik}\}$ , satisfying:

1.  $g_{ik}(a_k) = g_{ik}(a_{k+1}) = 0$
2.  $\theta_{ik}(a_k) = \theta_{ik}(a_{k+1}) = 0$
3.  $\|\theta_{ik} - \theta_{jk}\|_\infty \geq \frac{2\delta_2}{1 + \frac{K^2\delta_2}{4}} = 2\varepsilon$ , for  $i \neq j$ .

Now concatenate sequences  $\{g_{ik}\}$  to construct distinct functions on  $[0, L']$ ,  $\{g_i\}$  for  $i = 1, \dots, 2^m$ , with arclength at most  $L$ , satisfying  $g_i'(0) = g_i'(L') = g_i(0) = g_i(L') = 0$ . A short calculation shows that  $m \preceq \frac{KL'}{\delta_2} \sim \frac{KL}{\varepsilon}$ .

Furthermore, these functions are  $2\varepsilon$ -separated as curves. For  $i \neq j$ , there exists some subinterval  $I = [a, a + \delta/K]$  where  $g_i'$  has slope  $K$  and  $g_j'$  has slope  $-K$ , and so  $|g_i'(a + \delta/K) - g_j'(a + \delta/K)| \geq 2\delta_2$ . Without loss of generality, we may take  $a = 0$ ,  $g_i'(x) = Kx$  and  $g_j'(x) = -Kx$ . Then, on  $I$ :

$$\begin{aligned} \rho(g_i, g_j) &\geq \rho((\delta_2/K, g_i(\delta_2/k)), g_j) \\ &\geq \min_x \frac{1}{\lambda} \left| \frac{\delta_2}{K} - x \right| + \left| \theta_i\left(\frac{\delta_2}{K}\right) - \theta_j(x) \right| \\ &= \min_x \frac{1}{\lambda} \left| \frac{\delta_2}{K} - x \right| + \left| \arctan g_i'\left(\frac{\delta_2}{K}\right) - \arctan g_j'(x) \right| \\ &\geq \min_x \frac{1}{\lambda} \left| \frac{\delta_2}{K} - x \right| + \frac{1}{1 + \frac{K^2\delta_2}{4}} \left| f_i'\left(\frac{\delta_2}{K}\right) - f_j'(x) \right|. \end{aligned}$$

The minimum of the last expression occurs where  $x = \delta_2/K$  (recalling  $\lambda < 1/K$ ), giving  $\rho(g_i, g_j) = |\theta_i(\frac{\delta_2}{K}) - \theta_j(\frac{\delta_2}{K})| \geq \frac{2\delta_2}{1+\frac{\kappa^2\delta_2}{4}} = 2\varepsilon$  as desired.

Finally, we return to our initial claim, constructing functions  $\{f_{ik}\}$  on  $I_k$  with the promised properties. Equivalently, we construct realizations of an  $n$ -step piecewise linear symmetric random walk  $f$  with slopes  $\pm 1$  satisfying  $\int f = 0$  and  $f(0) = f(n) = 0$ . Let  $w$  be an  $\tilde{n}$ -step piecewise linear symmetric random walk,  $\tilde{n} < n$ , with  $w(0) = 0$  and slopes  $\pm 1$ . Set  $a(\tilde{n}) = \int_0^{\tilde{n}} w$ , and define the random variable  $z = \langle w(\tilde{n}), a(\tilde{n}) \rangle \Sigma \langle w(\tilde{n}), a(\tilde{n}) \rangle^T$ , where  $\Sigma$  is the covariance matrix of  $\langle w(\tilde{n}), a(\tilde{n}) \rangle$ .

If  $\{\epsilon_i\}_1^{\tilde{n}}$  is a collection of random variables taking on values  $\pm 1$  with equal probability, then  $w(\tilde{n}) = \sum_1^{\tilde{n}} \epsilon_i$  and  $a(\tilde{n}) = \sum_1^{\tilde{n}} (\tilde{n} - i + \frac{1}{2})\epsilon_i$ , giving:

$$\Sigma = \begin{bmatrix} \tilde{n} & \frac{\tilde{n}^2}{2} \\ \frac{\tilde{n}^2}{2} & \frac{\tilde{n}^3}{3} - \frac{\tilde{n}}{12} \end{bmatrix}.$$

Then  $E(z) = 2$  and

$$z = \frac{(4\tilde{n}^2 - 1)w(\tilde{n})^2 - 12\tilde{n}w(\tilde{n})a(\tilde{n}) + 12a^2}{\tilde{n}^3 - \tilde{n}}.$$

By the Markov inequality,  $P(z \leq 3) \geq 1/3$ , so at least a third of the total number  $2^{\tilde{n}}$  of distinct random walks  $w$  end at a point  $w(\tilde{n})$  within  $3\sqrt{\tilde{n}}$  steps of the  $x$ -axis, with area  $a(\tilde{n}) \leq \frac{\sqrt{3}}{2}\sqrt{4\tilde{n}^3 - \tilde{n}}$ . Denote this subset of random walks by  $\{\tilde{f}_i\}$ .

We now “complete” each  $\tilde{n}$ -step walk  $\tilde{f}_i$  to an  $n$ -step walk  $f_i$  with the desired properties. WLOG, take  $\tilde{f}_i(\tilde{n}) \geq 0$ . Certainly, the number of steps required to return to the  $x$ -axis is bounded above by  $3\sqrt{\tilde{n}}$ , adding at most  $9\tilde{n}/2$  in positive area. Now correct for area by adding steps to form triangles with the  $x$ -axis of base width  $b_k \in \mathbb{Z}^+$  steps, height  $b_k/2$  and area  $b_k^2/4$ . These steps must correct for an area of  $4 \times a(\tilde{n} + \tilde{f}_i(\tilde{n})) = \sum_k b_k^2$ , obtained in  $\sum_k b_k$  steps for the appropriate choice of  $\{b_k\}$ . Note that because any integer may be expressed as the sum of four squares [20],  $4 \times a(\tilde{n} + \tilde{f}_i(\tilde{n})) = b_1^2 + b_2^2 + b_3^2 + b_4^2$ . Because each  $b_k \leq 2\sqrt{a(\tilde{n} + \tilde{f}_i(\tilde{n}))}$ , the number of steps required to adjust the area satisfies:

$$\sum_{k=1}^4 b_k \leq 8\sqrt{\frac{9\tilde{n}}{2} + \frac{\sqrt{3}}{2}\sqrt{4\tilde{n}^3 - \tilde{n}}}.$$

Set  $n = \lceil \frac{KL}{\varepsilon} \rceil$ , and  $\tilde{n} = n - 2\sqrt{n} - 2\sqrt{\frac{9n}{2} + \frac{\sqrt{3}}{2}\sqrt{4n^3 - n}}$ . Then as  $\varepsilon \rightarrow 0$ ,  $n \rightarrow \infty$  and  $n/\tilde{n} \rightarrow 1$ , which, in counting the number of resulting  $\{f_i\}$ , completes the proof.  $\square$

To construct a  $2\varepsilon$ -separated set in  $\mathcal{J}_K^L$ , we follow much the same strategy as in the proof for Proposition 7, but now we join two halves of a circle of radius  $1/K$

with the primitive functions  $\{g_i\}$  to ensure the resulting curves are closed. As a result, we lose  $2\pi/K$  in arclength, and the tightness of the lower bound. Though we could not prove it, we believe the true constant in the lower bound should be  $KL$ .

We omit details of the proof of Proposition 8, as it is quite similar to the proof of Proposition 7.

**PROPOSITION 8.** *There exists a  $2\varepsilon$ -separated set for  $(\mathcal{I}_K^L, \rho)$  with  $\mathcal{M}_{2\varepsilon}^L$  elements, where  $\mathcal{M}_{2\varepsilon}^L \succeq 2^{\lfloor (KL-2\pi)/\varepsilon \rfloor}$ .*

Putting the pieces together, we have:

**THEOREM 9.**

- (a)  $\mathcal{H}_\varepsilon(\mathcal{C}_K^L, \rho) \sim \frac{KL}{\varepsilon}$ .
- (b)  $\mathcal{H}_\varepsilon(\mathcal{I}_K^L, \rho) \asymp \frac{1}{\varepsilon}$ .

#### 4. EFFICIENCY OF MEDIAL AXIS REPRESENTATION FOR COMPACT CURVE CLASSES

##### 4.1. Preliminaries

As we have seen in Section 3, the leading order term in the  $\varepsilon$ -entropy for the compact classes of boundary curves comes from  $\varepsilon$ -covering the corresponding classes of tangent angle functions. We see that, because  $\theta_\gamma = \theta_m \pm \phi + \pi/2$ , the construction of a medial-axis-based  $\varepsilon$ -covering for a compact class of curves requires  $\varepsilon/2$ -coverings for the associated classes of  $\{\theta_m\}$  and  $\{\phi\}$ . Doing this for all possible medial branches for boundary curves  $\gamma \in \mathcal{E}_K^L$  and then counting the number of possible configurations of medial branches would produce an  $\varepsilon$ -covering for the class of boundary curves. Already, however, we find trouble: the space  $\mathcal{E}_K^L$  is too large for the medial axis to efficiently approximate. For example, a boundary curve with arbitrarily many maxima of curvature would require a medial axis with arbitrarily many branches, and so a medial  $\varepsilon$ -covering would not be finite. Closer investigation shows that there are three ways the medial axis for  $\gamma \in \mathcal{E}_K^L$  can be badly behaved, illustrated in Figure 5. We will therefore restrict to the class  $\mathcal{E}_K^M$ , defined below.

**DEFINITION.** *Let  $\mu, v$  be constants satisfying  $0 < v < 1$ ,  $\mu \in (0, \frac{\pi}{2})$ . Define  $\mathcal{E}_K^M = \mathcal{E}_K^M(\mu, v)$  as the collection of generic  $C^2$  curves  $\gamma \in \mathcal{E}$  satisfying the following properties:*

- (a)  $|\kappa_\gamma| \leq K$ .
- (b)  $\kappa_\gamma$  has at most  $\frac{M+3}{2}$  local maxima.
- (c)  $r \geq \frac{1}{K}$  (which implies  $\kappa_\gamma \leq K$ , but not  $\kappa_\gamma \geq -K$ ).
- (d) If  $\phi \in [\mu, \pi - \mu]$ , then  $\kappa_\gamma \geq 0$  and  $1 - r\kappa_\gamma \geq v$ .
- (e) If  $\phi < \mu$  or  $\phi > \pi - \mu$ , then  $\kappa_\gamma > 0$  and  $|1 - r\kappa_\gamma| \rightarrow 0$  monotonically towards a vertex of  $\gamma$  where the medial circle osculates.

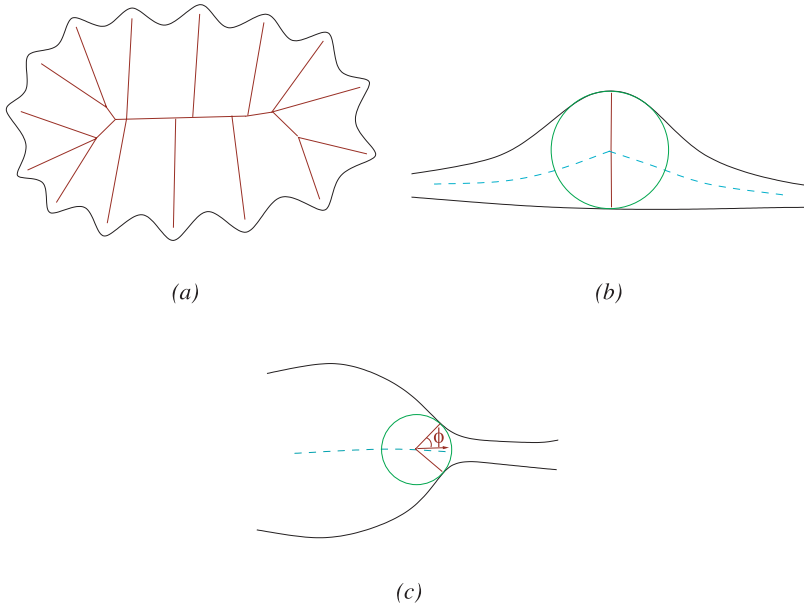


Figure 5. Types of boundary curves where the medial axis is badly behaved: (a) arbitrarily many branches in the medial axis; (b) axis sensitivity to small boundary perturbations causing a new branch to sprout at the “kink” in the medial curve where a bitangent circle is arbitrarily close to osculating; (c) apparent approach to boundary curve vertex that instead funnels into a narrow tube.

Property (a) comes from the curvature bound in our original class  $\mathcal{E}_K^I$ . Property (b) restricts the number of branches in a medial curve. Property (c) requires that points on opposite sides of the boundary curve remain properly separated (and  $\gamma$  therefore robustly an embedding). Property (d) restricts how close a medial circle can come to osculating via the parameter  $\nu$ , which also controls the relationship between the boundary and medial curve arclength parameters,  $\frac{ds_{\pm}}{d\nu} = \frac{\mp\sqrt{1-r^2}}{1-r\kappa_{\pm}}$ . Property (e) and its parameter  $\mu$  control values for  $\phi$  for points away from boundary vertices where the medial circle osculates. In addition, the monotonicity condition ensures the boundary curve is well-behaved in a neighborhood around each vertex.

Property (e) also naturally decomposes each medial branch into an *interior region* where  $\phi \in [\mu, \pi - \mu]$ , and an *endpoint region* where  $\phi < \mu$  or  $\phi > \pi - \mu$ . The endpoint regions correspond to portions of a medial curve near an axis endpoint where the medial circle osculates with fourth-order contact at a local maximum of curvature for  $\gamma$ . See Figure 6. Interior and endpoint regions often require different treatments, as may be seen in the need for Damon’s edge operator [5] and Giblin and Kimia’s treatment in [8]. Our approach continues the tradition.

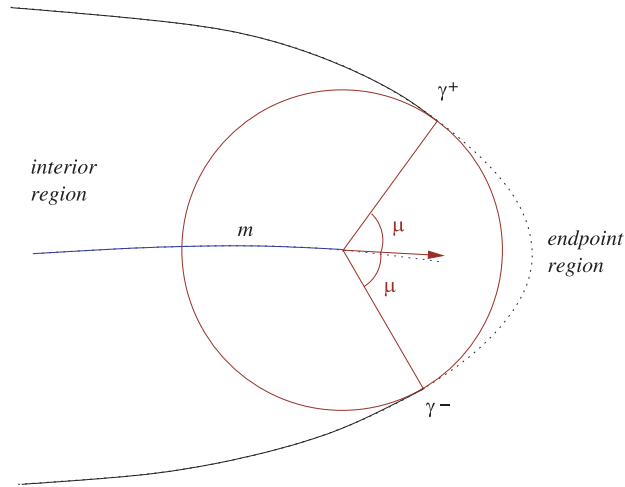


Figure 6. Interior and endpoint regions of a curve.

PROPOSITION 10.  $\mathcal{E}_K^M$  is totally bounded in the metric  $\rho$ .

PROOF. If the length of  $\gamma \in \mathcal{E}_K^M$  is uniformly bounded, then there exists an  $L$  so that  $\mathcal{E}_K^M$  is a subset of  $\mathcal{I}_K^L$ , and is therefore totally bounded.

Assume no such  $L$  exists. Consider the function  $f(s, t) = \gamma(s) + t\mathbf{N}(s)$ , where  $s$  is arclength on  $\gamma$  and  $\mathbf{N}$  is the inward pointing normal direction. Since  $r \geq \frac{1}{K}$ , for  $0 \leq t < \frac{1}{K}$  and  $\gamma \in \mathcal{E}_K^M$ , the map  $\gamma(s) \rightarrow f(s, t)$  is injective. For  $\gamma$  of length  $l$ , the area  $A(l)$  of the region with boundary  $\gamma$  is therefore at least as large as the area of the region between  $\gamma$  and  $f(s, t_\delta)$ , where  $t_\delta = \frac{1}{K+\delta}$  for some fixed  $\delta > 0$ . See Figure 7. Computing the Jacobian of  $f$ , we therefore have:

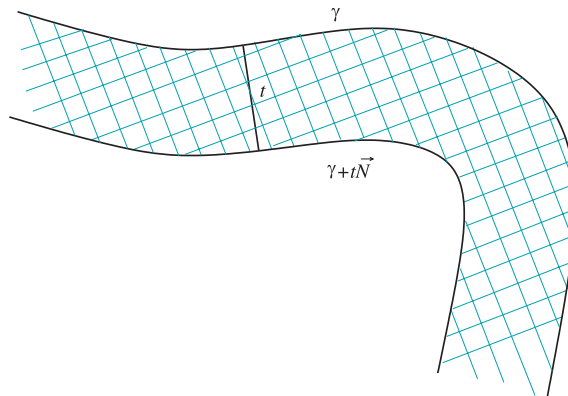


Figure 7. Minimum area inside a curve  $\gamma \in \mathcal{E}_K^M$ .

$$\begin{aligned}
A(l) &\geq \int_0^{t_\delta} \int_0^l 1 - \kappa_\gamma t \, ds \, dt \\
&\geq \int_0^{t_\delta} \int_0^l 1 - Kt \, ds \, dt \\
&= l \int_0^{t_\delta} 1 - Kt \, ds \, dt \\
&= l \left( \frac{1}{K + \delta} - \frac{K}{2(K + \delta)^2} \right).
\end{aligned}$$

As  $l \rightarrow \infty$ ,  $A(l) \rightarrow \infty$ , violating the boundedness of  $\Omega$ . Therefore, an upper bound  $L$  for the lengths of curves  $\gamma \in \mathcal{E}_K^M$  must exist.  $\square$

Note that the boundedness of  $\Omega$  also ensures the existence of an  $\bar{R}$  so that  $r \leq \bar{R}$  for all medial circles, an observation which allows us to prove that when medial data for two boundary curves are close, the curves themselves must also be close.

**PROPOSITION 11.** *Suppose  $(m_i(v), r_i(v))$ ,  $v \in [0, l]$ , are  $C^1$  medial branches for  $\gamma_i$ , a boundary curve with tangent angle functions  $\theta_i$ , and inward-pointing normal vectors  $\mathbf{N}_i$ ,  $i = 1, 2$ . Then:*

$$\begin{aligned}
\rho(\gamma_1, \gamma_2) &\leq \sup_v \frac{1}{\lambda} (|m_1 - m_2| + |r_1 - r_2| + \bar{R}(|\theta_{m_1} - \theta_{m_2}| + |\phi_1 - \phi_2|)) \\
&\quad + |\theta_{m_1} - \theta_{m_2}| + |\phi_1 - \phi_2|.
\end{aligned}$$

**PROOF.**

$$\begin{aligned}
\rho(\gamma_1, \gamma_2) &\leq \sup_v \frac{1}{\lambda} |\gamma_1(v) - \gamma_2(v)| + |\theta_1(v) - \theta_2(v)| \\
&= \sup_v \frac{1}{\lambda} (|m_1 + r_1 \mathbf{N}_{\gamma_1} - m_2 - r_2 \mathbf{N}_{\gamma_2}|) + |\theta_{m_1} + \phi_1 - \theta_{m_2} - \phi_2| \\
&\leq \sup_v \frac{1}{\lambda} (|m_1 - m_2| + |r_1 \mathbf{N}_{\gamma_1} - r_2 \mathbf{N}_{\gamma_2}|) + |\theta_{m_1} - \theta_{m_2}| + |\phi_1 - \phi_2| \\
&\leq \sup_v \frac{1}{\lambda} (|m_1 - m_2| + |r_1 - r_2| + \bar{R} |\mathbf{N}_{\gamma_1} - \mathbf{N}_{\gamma_2}|) \\
&\quad + (|\theta_{m_1} - \theta_{m_2}| + |\phi_1 - \phi_2|) \\
&\leq \sup_v \frac{1}{\lambda} (|m_1 - m_2| + |r_1 - r_2| + \bar{R} (|\theta_{m_1} - \theta_{m_2}| + |\phi_1 - \phi_2|)) \\
&\quad + |\theta_{m_1} - \theta_{m_2}| + |\phi_1 - \phi_2| \quad \square
\end{aligned}$$

In fact, as we demonstrate in [13], one can prove that if two medial points are close along the interior of a medial curve, the possible location of intermediate

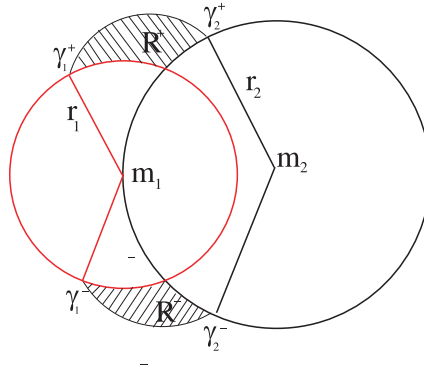


Figure 8. Possible regions  $R^+$  and  $R^-$  for boundary points given medial data points  $(m_1, r_1), (m_2, r_2)$ .

boundary points is small. Because of the geometry of the medial construction, namely that the medial circles are maximal and contained entirely within the boundary curve, the boundary must lie in a region defined by the location of possible intermediate medial circles, as illustrated by Figure 8.

#### 4.2. Covering Medial Curves for Interior Regions

To apply the upper bound for the  $\varepsilon$ -entropy for  $\mathcal{C}_K^L$  in Theorem 9 to construct a covering for the interiors of the medial branches, we must first compute a bound on the arclength and on the Lipschitz constant for the tangent angle function for an interior curve.

**PROPOSITION 12.** *There exists a constant  $L_m$  so that for  $m$ , a single branched medial curve interior for  $\gamma \in \mathcal{E}_K^M$  of length  $l$ ,  $l \leq L_m$ .*

**PROOF.** Parameterizing  $m$  by  $s_+$ , for  $m$  corresponding to  $\gamma_{\pm}$ , we have:

$$\begin{aligned}
 l &\leq \int_0^L \left| \frac{dv}{ds_+} \right| ds_+ \\
 &= \int_0^L \left| \frac{1 - r\kappa_+}{\sqrt{1 - r'^2}} \right| ds_+ \\
 &\leq \int_0^L \frac{1 + K\bar{R}}{\sin \mu} ds_+ \\
 &\leq \frac{L(1 + K\bar{R})}{\sin \mu} \\
 &= L_m.
 \end{aligned}$$

□

LEMMA 13. Suppose  $m(v)$  is the interior of a medial curve for a boundary curve  $\gamma \in \mathcal{E}_K^M$ , with tangent angle function  $\theta_m(v)$ .  $\theta_m(v)$  is Lipschitz with:

$$|\theta_m(v_1) - \theta_m(v_2)| \leq \frac{K}{v} |v_1 - v_2|.$$

PROOF. From Equation 3 we have:

$$\begin{aligned} \left| \frac{d\theta_m}{dv} \right| &= \left| \frac{1}{2} \sin\left(\frac{\theta_+ - \theta_-}{2}\right) \left( -\frac{\kappa_+}{1 - r\kappa_+} + \frac{\kappa_-}{1 - r\kappa_-} \right) \right| \\ &\leq \frac{1}{2} \left( \frac{K}{v} + \frac{K}{v} \right) \\ &= \frac{K}{v}. \end{aligned}$$

PROPOSITION 14. Let  $\mathcal{M}$  denote the class of medial interiors for medial axes associated to curves in  $\mathcal{E}_K^M$ . There exists a  $(\frac{\sqrt{\delta^3}}{\lambda} + \delta)$ -cover for  $(\mathcal{M}, \rho)$  with at most  $N_\delta$  elements, where:

$$N_\delta \leq 2^{KL_m M / v\delta}$$

elements.

PROOF. We will construct a cover for  $\mathcal{M}$  by covering the class of possible interior branches,  $\mathcal{M}_0$ , then piecing together branch approximations to form axis configurations. By Lemma 1, since  $\kappa_\gamma$  has at most  $\frac{M+3}{2}$  local maxima of curvature, any axis configuration  $\mathbf{m}$  has at most  $M$  branches.

First, approximate the arclength parameters of medial curve interiors. Partition the interval of possible interior arclengths,  $[0, L_m]$ , into subintervals  $I_k = (l_k - \frac{\delta^\xi}{4}, l_k]$ , for  $k = 1, \dots, \lceil \frac{4L_m}{\delta^\xi} \rceil$  and  $\xi > 1$ . Parameterize an interior curve  $m$  of length  $l \in I_k$  by  $v_k$ , where  $\frac{dv}{dv_k} = \frac{l}{l_k}$  and  $v$  is arclength on  $m$ . Take  $\xi = \frac{3}{2}$ . Note that because  $l \leq l_k$ ,  $\left| \frac{d\theta_m}{dv_k} \right| \leq \left| \frac{d\theta_m}{dv} \right|$ , and so the curvature bound in Lemma 13 still holds.

Next, apply Kolmogorov's Corollary 3 together with Lemma 13 for each of the  $\lceil \frac{4L_m}{\delta^\xi} \rceil$  length subintervals  $I_k$  to find an  $L^\infty$   $\delta$ -cover of the tangent angles to medial interiors with at most:

$$\left( 2 \left\lceil \frac{\pi}{2\delta} \right\rceil + 1 \right) \left\lceil \frac{4L_m}{\delta^\xi} \right\rceil 2^{\lceil KL_m / v\delta \rceil}$$

elements. By Proposition 6, we then have a  $(\frac{\sqrt{\delta^3}}{\lambda} + \delta)$ -cover for the class of medial interior curves in the metric  $\rho$  with at most:

$$\left( 2 \left\lceil \frac{\pi}{2\delta} \right\rceil + 1 \right) \left\lceil \frac{4L_m}{\sqrt{\delta^3}} \right\rceil 2^{\lceil KL_m / v\delta \rceil + \log 3 \lceil 4L_m / \sqrt{\delta} \rceil}$$

elements.

Assemble the cover for branch interiors into a cover for interior axis configurations. Our approximations will consist of all possible combinations of interior branch approximations where a new branch is joined to a configuration at one of three equally spaced points at a distance of  $\frac{\sqrt{\delta^3}}{2}$  from the end of the previous branch (in the spirit of Figure 4). As there are at most  $M$  branches,

$$\left\lceil \frac{4L_m}{\sqrt{\delta^3}} \right\rceil 2^{\lceil KL_m/v\delta \rceil + \log 3 \lceil 4L_m/\sqrt{\delta} \rceil} + 1$$

choices for each branch (including the choice of no branch), and three choices for where to attach each branch, we have a cover for  $\mathcal{M}$  with no more than:

$$3 \left( 2 \left\lceil \frac{\pi}{2\delta} \right\rceil + 1 \right) \left\lceil \frac{4L_m}{\sqrt{\delta^3}} \right\rceil 2^{\lceil KL_m M/v\delta \rceil + \log 3 \lceil 4L_m/\sqrt{\delta} \rceil} + 1$$

branches.

Finally, we verify that our cover is indeed a  $(\frac{\sqrt{\delta^3}}{\lambda} + \delta)$ -cover in the metric  $\rho$ . For  $\gamma \in \mathcal{E}_K^M$  with medial axis  $\mathbf{m}$ , orient  $\mathbf{m}$  so that a branch containing an endpoint region has interior beginning at the origin. Denote this branch  $m_0$ . Then there exists  $m_{0,\delta}$  in the cover for medial interior curves so that (positioning  $m_{0,\delta}$  at the origin)  $|m_0(0) - m_{0,\delta}(0)| \leq \frac{\sqrt{\delta^3}}{2}$ , and within the branch,  $\rho(m_0, m_{0,\delta}) \leq (\frac{\sqrt{\delta^3}}{\lambda} + \delta)$ . At the end of  $m_0$  other branches may join. Select the next branch,  $m_1$ , and its approximation,  $m_{1,\delta}$ . Positioning  $m_{1,\delta}$  at the choice of three starting points that minimizes  $|m_{1,\delta}(0) - m_1(0)|$  guarantees that  $|m_1(0) - m_{1,\delta}(0)| \leq \frac{\sqrt{\delta^3}}{2}$ , and therefore  $\rho(m_1, m_{1,\delta}) \leq (\frac{\sqrt{\delta^3}}{\lambda} + \delta)$ . At the endpoint of  $m_{1,\delta}$ , we repeat. Inductively, this gives our approximation to  $\mathbf{m}$  as a member of the constructed cover, satisfying for the  $i^{\text{th}}$  branch  $\rho(m_i, m_{i,\delta}) \leq (\frac{\sqrt{\delta^3}}{\lambda} + \delta)$ .  $\square$

### 4.3. Covering Radius Functions for Interior Regions

Recalling that  $\frac{dr}{dv} = -\cos \phi$ , we construct an  $L^\infty$  cover for the derivatives of the radius functions by covering the class  $\Phi = \{\phi\}$  associated to  $\mathcal{E}_K^M$ .

LEMMA 15. *There exists a  $\delta$ -net  $\Phi_\delta$  for  $(\Phi, L^\infty)$  with at most  $(2 \lceil \frac{\pi}{4\delta} \rceil + 1) 2^{\lceil KL_m/v\delta \rceil}$  elements.*

PROOF. To apply Kolmogorov's Corollary 3, we need only show that the class  $\Phi$  is Lipschitz as a function of  $v_k$  (as defined in the proof of Proposition 14). Equation 4 gives:

$$\begin{aligned}
\left| \frac{d\phi}{dv_k} \right| &= \left| \frac{d\phi}{dv} \right| \left| \frac{dv}{dv_k} \right| \\
&= \frac{l}{l_k} \left| \frac{d\phi}{dv} \right| \\
&\leq \left| \frac{d\phi}{dv} \right| \\
&= \left| \frac{1}{2} \sin\left(\frac{\theta_+ - \theta_-}{2}\right) \left( \frac{\kappa_+}{1 - r\kappa_+} + \frac{\kappa_-}{1 - r\kappa_-} \right) \right| \\
&\leq \frac{1}{2} \left( \frac{K}{v} + \frac{K}{v} \right) \\
&= \frac{K}{v}. \quad \square
\end{aligned}$$

By Theorem 4, Lemma 15 produces a  $(\frac{\sqrt{\delta^3}}{\lambda} + \delta)$ -cover for the radius functions:

**PROPOSITION 16.** *For  $\xi > 1$ , there exists a  $(\frac{\sqrt{\delta^3}}{\lambda} + \delta)$ -covering in the metric  $\rho$  for the class of radius functions associated to the interiors of  $\mathcal{E}_K^M$  with no more than:*

$$\left( 2 \left\lceil \frac{\pi}{4\delta} \right\rceil + 1 \right) \left\lceil \frac{R}{\delta^\xi} \right\rceil 2^{[KL_m/v\delta] + [l_k/\delta^{\xi-1}] + 2}$$

elements.

**PROOF.** Note that if  $|\phi - \phi_\delta| < \delta$ ,  $|\cos \phi - \cos \phi_\delta| < \delta$ . Hence a  $\delta$ -cover for  $\Phi$  gives a  $\delta$ -cover for  $\{r'(v)\}$ .

Construct a  $\delta^\xi$ -net for the interval  $[\frac{1}{K}, \bar{R}]$  of possible values for  $r(0)$ , with at most  $\lceil \frac{R}{\delta^\xi} \rceil$  elements. For each of these initial values, apply the results of Theorem 4 with a derivative  $r'$  approximated by  $\cos \phi_\delta$  for the appropriate center of a  $\delta$ -ball,  $\phi_\delta$ , in the covering constructed in Lemma 15. The number of elements in the resulting cover is as claimed.  $\square$

#### 4.4. Covering Interior Regions for $\gamma \in \mathcal{E}_K^M$

The necessary pieces are now in place to construct an  $\varepsilon$ -covering for the interior regions of boundary curves in  $\mathcal{E}_K^M$ .

**PROPOSITION 17.** *There exists a medial axis-based  $\varepsilon$ -cover for the collection of curve interiors for  $\mathcal{E}_K^M$  with at most  $\mathcal{N}_\varepsilon$  elements, where:*

$$\mathcal{N}_\varepsilon \preceq 2^{(2KL_m M/v\varepsilon)(2\bar{R}/\lambda + 2)}.$$

**PROOF.** Choose  $\delta$  so that  $\varepsilon = \frac{2\sqrt{\delta^3}}{\lambda} + (\frac{2\bar{R}}{\lambda} + 2)\delta$ , giving  $\lim_{\varepsilon \rightarrow 0} \frac{\varepsilon}{\delta} = \frac{2\bar{R}}{\lambda} + 2$ . Take  $\xi = 3/2$  in Proposition 14 and Lemma 15.

Construct  $(\frac{\sqrt{\delta^3}}{\lambda} + \delta)$ -coverings for the interior medial axes and radius functions as above. From these, construct a covering of the interior regions of the boundary curves so that two boundary curves are in the same ball when the corresponding axes and radius functions are in the same ball in their respective  $(\frac{\sqrt{\delta^3}}{\lambda} + \delta)$ -coverings. We claim the resulting covering of boundary interior regions has diameter at most  $2\varepsilon$ .

Suppose  $\gamma$  and  $\tilde{\gamma}$  are in the same ball, with interior medial branches and radius functions  $\{(m_i, r_i)\}$ ,  $\{(\tilde{m}_i, \tilde{r}_i)\}$  and associated angle functions  $\{(\theta_i, \phi_i)\}$ ,  $\{(\tilde{\theta}_i, \tilde{\phi}_i)\}$  respectively. Let  $\{v_i\}$  be the approximated arlength parameters for each medial branch as defined in the proof of Proposition 14 (with slight abuse of notation). Then:

$$\begin{aligned} \rho(\gamma_1, \gamma_2) &\leq \sup_i \sup_{v_i} \frac{1}{\lambda} (|m_i(v_i) - \tilde{m}_i(v_i)| + |r_i(v_i) - \tilde{r}_i(v_i)| + \bar{R}(|\phi_i(v_i) - \tilde{\phi}_i(v_i)| \\ &\quad + |\theta_i(v_i) - \tilde{\theta}_i(v_i)|)) + |\phi_i(v_i) - \tilde{\phi}_i(v_i)| + |\theta_i(v_i) - \tilde{\theta}_i(v_i)| \\ &\leq \frac{2}{\lambda} (2\sqrt{\delta^3} + 2\bar{R}\delta) + 4\delta \\ &= 2\varepsilon. \end{aligned} \quad \square$$

#### 4.5. Covering Endpoint Regions

It remains to construct a covering for the endpoint regions. The leading term in the expression for  $\varepsilon$  in terms of  $\delta$  is Proposition 17 is  $(2 + \frac{2\bar{R}}{\lambda})\delta$  and so we require only  $\delta' = (2 + \frac{2\bar{R}}{\lambda})\delta$  accuracy to cover the tangent angle functions is the endpoint region boundary curves in order to match the accuracy obtained for the curve interiors. Recall that in the endpoint regions,  $\phi < \mu$  or  $\phi > \pi - \mu$ ,  $\kappa_\gamma > 0$ , and  $|1 - r\kappa_\gamma| \rightarrow 0$  monotonically.

In the endpoint regions, because  $\kappa_\gamma > 0$  monotonically increases as corresponding points on the axis curve approach the axis endpoint,  $\gamma$  is contained entirely within the region defined by the tangent lines to  $\gamma$  at the points  $\gamma_\pm^\mu$  and the medial circle joining  $\gamma_+^\mu$  and  $\gamma_-^\mu$ . See Figure 9. This gives a maximum value of  $2\bar{R}\tan\mu$  for the arlength of the endpoint region of the boundary curve. Therefore, application of Proposition 6 produces a  $(\delta' + \frac{\sqrt{\delta'^3}}{\lambda})$ -cover for endpoint regions with at most:

$$\left\lceil \frac{8\bar{R}\tan\mu}{\sqrt{\delta'^3}} \right\rceil 2^{[2K\bar{R}\tan\mu/\delta'] + \log 3[8\bar{R}\tan\mu/\sqrt{\delta'}]}$$

elements.

Take  $\varepsilon = \frac{2\sqrt{\delta^3}}{\lambda} + (2 + \frac{2\bar{R}}{\lambda})\delta$  as in the previous section, so  $\frac{\delta'}{\varepsilon} \rightarrow 1$ .

**PROPOSITION 18.** *For endpoint regions of curves  $\gamma \in \mathcal{E}_K^M$ , there exists an  $\varepsilon$ -cover in the metric  $\rho$  with  $M_\varepsilon$  elements, where:*

$$M_\varepsilon \preceq 2^{2K\bar{R}\tan\mu/\varepsilon}.$$

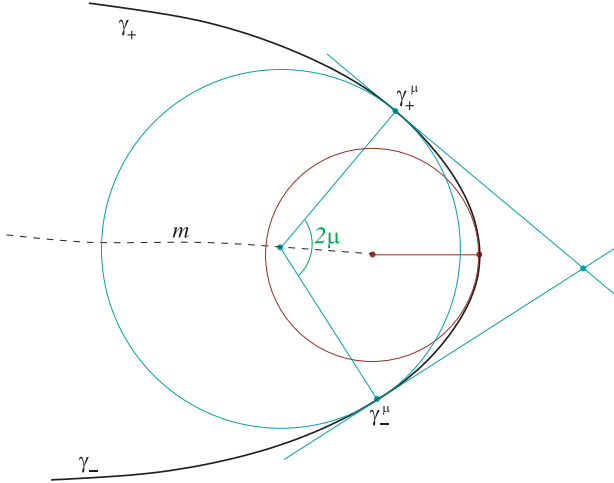


Figure 9. Bounded area for possible endpoint regions of the boundary curve.

4.6. Medial-axis Based  $\varepsilon$ -covering Theorem

**THEOREM 19.** *There exists a medial axis-based  $\varepsilon$ -cover for  $(\mathcal{E}_K^M, \rho)$  with at most  $K_\varepsilon$  elements, where:*

$$K_\varepsilon \preceq 2^{(M/\varepsilon)(2K\bar{R}\tan\mu+(2KL_m/v)(2\bar{R}/\lambda+2))}.$$

**PROOF.** We apply Proposition 18 to each of at most  $M$  endpoint regions. This, together with Proposition 17, proves the theorem.  $\square$

The order of  $\varepsilon$  in Theorem 19 is certainly correct. In any realistic setting, however, the appropriate constant  $KL$  in Theorem 9 will be smaller than the constant in Theorem 19. It is possible we could improve the exponent some, but Lemmas 13 and 15 suggest a lower bound for the exponent of  $4KL_mM\bar{R}$ , which is still likely to be larger than  $KL$  in all but exceptional cases. In other words, a medial-axis-based  $\varepsilon$ -covering (or, equivalently, uniform encoding) for compact classes of curves is sub-optimal.

5. EFFICIENCY OF MEDIAL AXIS REPRESENTATION FOR NON-COMPACT CURVE CLASSES

It turns out that adaptive encoding is where the strengths of the medial axis hold forth. As we have seen above, the high order terms in encoding curves for both boundary and medial axis encodings comes from the encoding of the angle functions,  $\{\theta_\gamma\}$  or  $\{(\theta_m, \phi)\}$ . The identity  $\theta_\gamma = \theta_m \pm \phi + \pi/2$  reveals that a uniform  $\varepsilon$ -encoding using the medial axis requires approximating both  $\phi$  and  $\theta_m$  to an accuracy of  $\varepsilon/2$ . In an adaptive strategy, error can be adaptively allocated to the

medial angle contributing the most to  $\theta_\gamma$ . The key ingredient to the proof of Theorem 21 is the relationship of medial geometry to boundary geometry captured in the next lemma.

LEMMA 20. *Let  $m$  be a branch of a medial curve of length  $l$  for  $\gamma \in \mathcal{E}$ . Let  $s$  be an arclength parameter for  $\gamma$  so that  $\gamma(s)|_{s \in D} = \gamma_+ \cup \gamma_-$  (so  $D$  is the appropriate subdomain for  $s$  corresponding to the medial branch  $m$ ). Then:*

$$\int_D |\kappa| ds = \int_{[0,l]} |\kappa_m| + |\phi'| + ||\kappa_m| - |\phi'||| dv.$$

Given this explicit relationship between the medial variation and the boundary variation, we can adaptively partition the  $\varepsilon$ -error into  $\eta$ -error for encoding  $\theta_m$  and  $(\varepsilon - \eta)$ -error for encoding the medial angles, where  $0 < \eta < \varepsilon$  is chosen to minimize codelength. Then, on one hand, Theorem 5 produces an encoding of length

$$L(\gamma) \preceq \frac{\int |\kappa_\gamma| ds + \delta}{\varepsilon}$$

for the boundary representation and, on the other, an encoding of length

$$\tilde{L}(\gamma) \preceq \frac{\int |\kappa_m| dv + \delta_1}{\eta} + \frac{\int |\phi'| dv + \delta_2}{\varepsilon - \eta}$$

for the medial representation. Introducing locally adaptive choices for  $\eta$  gives the result in Theorem 21.

THEOREM 21. *Let  $m$  be an arclength parameterized medial branch defined on a closed interval  $I$  for  $\gamma \in \mathcal{E}$  with corresponding boundary segments  $\gamma_\pm$ . Then encoding  $\gamma_\pm$  via the medial axis is more efficient than directly adaptively encoding  $\theta_\gamma$  whenever  $I$  can be partitioned into a finite number of subintervals  $I_j$  where for each  $j$ :*

$$\frac{\sup_{I_j} |\kappa_m|}{\sup_{I_j} |\phi'|} > 3 + \sqrt{8} \quad \text{or}$$

$$\frac{\sup_{I_j} |\phi'|}{\sup_{I_j} |\kappa_m|} > 3 + \sqrt{8}.$$

PROOF. Following the proof of Theorem 5, select  $g_\kappa$  and  $\delta_1$  satisfying  $|\kappa_m| \leq g_\kappa$  and  $\int g_\kappa \leq \int |\kappa_m| + \delta_1$ , and select  $g_\phi$  and  $\delta_2$  satisfying  $|\phi'| \leq g_\phi$  and  $\int g_\phi \leq \int |\phi'| + \delta_2$ . Construct an encoding scheme as follows. Partition  $I$ , the domain of  $m$ , into maximal subdomains  $\{I_j\}$  on which both  $g_\kappa$  and  $g_\phi$  are constant. Since both functions are piecewise constant with a finite number of jumps, the number of such subdomains will be finite. On each subdomain, compute the minimizing  $\eta_j$ . Then the medial axis will be more efficient when:

$$g_\kappa + g_\phi + 2\sqrt{g_\kappa g_\phi} < 2 \max\{g_\kappa, g_\phi\}.$$

For  $g_\kappa \geq g_\phi$ , this gives:

$$\frac{g_\kappa}{g_{\phi'}} > 3 + \sqrt{8},$$

otherwise take the reciprocal of the left side of the inequality. Recalling the construction of the functions  $g_\kappa$  and  $g_\phi$ , the result is proved.  $\square$

In other words, the medial axis will be more efficient when either  $\phi$  or  $\theta_m$  contributes significantly to the variation of  $\theta_\gamma$ , but not both.

## 6. DISCUSSION

Theorem 21 partitions the noncompact class of embeddings with Lipschitz tangent angle into two subclasses: those for which the boundary is more efficient and those for which the medial axis is more efficient. In [12, 13], we returned to our motivating problem of shape modeling and analyzed efficiency of representation for 2322 shapes [16, 18, 21], in order to characterize a shape by whether the boundary or medial axis was more efficient.

Our results show only three shapes for which the boundary was a better choice. It seems that for curves bounding shapes of interest to humans, the branches of the medial axis tend to be nearly straight, and almost all the geometry of the boundary is captured by the angle  $\phi$ . Figure 10 shows the two shapes for which the boundary representation gave maximum efficiency improvement, while Figure 11 shows the two shapes for which the medial representation gave maximum efficiency improvement. While it appears that pixelation effects are a likely explanation for why the boundary is more efficient for the shapes in Figure 10, further exploration is required to completely characterize shapes that will be more efficiently modeled by the boundary curve.

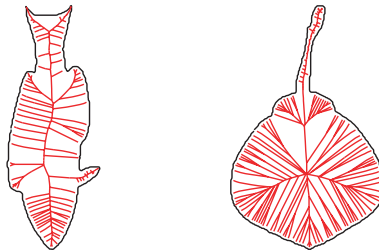


Figure 10. Two shapes for which the boundary was maximally efficient, out of three shapes total where the boundary outperformed the medial axis. Fish: boundary encoding rate 58% of medial axis rate. Stingray: boundary rate 20% of medial axis rate. Pixelation effects are a likely explanation for the boundary's greater efficiency. Note how dense the axis branches are for the stingray. Not visible in the fish image are many very short axis branches along the tips of branches going into fins.

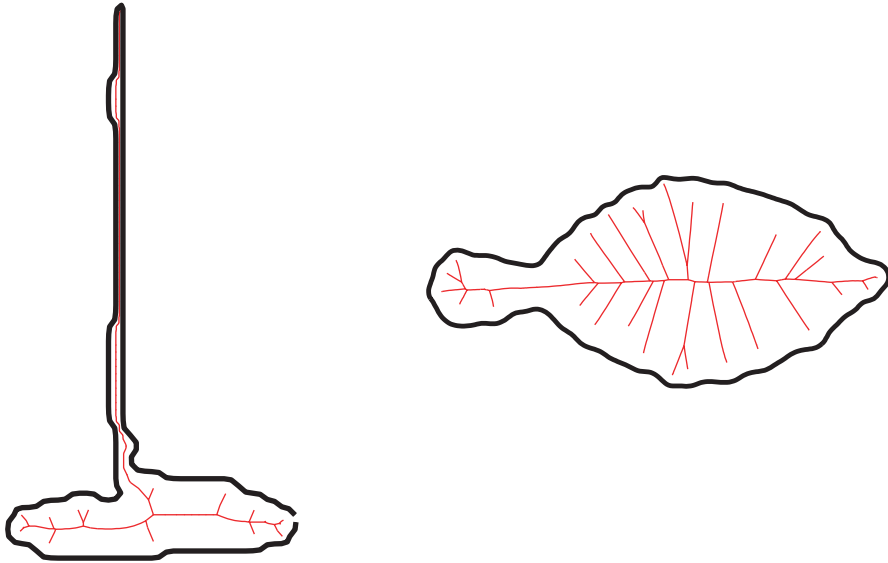


Figure 11. Two shapes for which the medial axis was maximally efficient. Sailboat: medial axis encoding rate 46% of boundary rate. Fish: medial axis rate 47% of boundary rate.

We have seen that the medial axis is most efficient when either the medial curve or the angle  $\phi$  encodes most of the geometry of the boundary curve. One generalization of the Blum medial axis, presented by Damon [5], is to broaden the class of medial curves beyond loci of maximal circles, and to replace the radius function with a multi-valued radial vector field on the medial curve. The relationship between the geometry of the medial axis and the boundary becomes more complicated, but in return the axis representation is less restrictive. Currently, we are exploring whether this generalization will allow for even greater efficiency, as we can, *e.g.*, choose medial curves with minimal curvature and encode most of the boundary geometry in the radial vector field.

#### REFERENCES

- [1] J. AUGUST - A. TANNENBAUM - S. ZUCKER. On the Evolution of the Skeleton. Preprint, 1999.
- [2] M. F. BEG - M. I. MILLER - A. TROUVE - L. YOUNES. Computing metrics via geodesics on flows of diffeomorphisms. International Journal of Computer Vision, July 2003.
- [3] H. BLUM. Biological shape and visual science. J. Theor. Biol. **38**:205–287, 1973.
- [4] E. BRONSTEIN.  $\varepsilon$ -entropy of convex sets and functions. Siberian Mathematics Journal **17**:393–398, 1976.
- [5] J. N. DAMON. Determining the geometry of boundaries of objects from medial data. IJCV, **63(1)**:45–64, 2005.

- [6] R. M. DUDLEY. Metric entropy of some classes of sets with differentiable boundaries. *J. Approx. Th.*, **10**:227–236, 1974.
- [7] M. FEISZLI. Conformal Shape Representation. PhD Thesis, Brown University, 2008.
- [8] P. GIBLIN - B. KIMIA. On the intrinsic reconstruction of shape from its symmetries. *IEEE Trans. on Pattern Anal. and App.* **25(7)**:895–911, 2003.
- [9] R. A. KATZ - S. M. PIZER. Untangling the Blum medial axis transform. *IJCV*, **55(2–3)**:139–153, 2003.
- [10] E. KLASSEN - A. SRIVASTAVA - W. MIO - S. JOSHI. Analysis of planar shapes using geodesic paths in shape space. *IEEE Trans. Pattern Analysis and Machine Intelligence*, **26**:372–383, 2004.
- [11] A. N. KOLMOGOROV - V. M. TIKHOMIROV.  $\varepsilon$ -entropy and  $\varepsilon$ -capacity. *American Mathematical Society Translations, Series 2*, **17**:277–364, 1959.
- [12] K. LEONARD, *An efficiency criterion for 2D shape model selection*, *IEEE CVPR Proc.*, **1**, 2006, 1289–1296.
- [13] K. LEONARD, *Efficient shape modeling:  $\varepsilon$ -entropy, adaptive coding, and Blum's medial axis versus the boundary curve*, *Int. J. Comp. Vis.*, **74**, 2007, 183–199.
- [14] K. LEONARD. Measuring Shape Space:  $\varepsilon$ -entropy, adaptive coding and 2-dimensional shape. PhD Thesis, Brown University, 2004.
- [15] J. MATHER. Distance from a manifold in Euclidean space. *Proc. Symp. Pure Math.*, **40(2)**:199–216, 1983.
- [16] D. MARTIN - C. FOWLKES - D. TAL - J. MALIK. A database of human segmented natural imaged and its application to evaluating segmentation algorithms and measuring ecological statistics. *Proc. 8th Int'l Conf. Computer Vision*, **2**:416–423, July 2001.
- [17] P. MICHOR - D. MUMFORD. Riemannian geometries on the space of plane curves. *J. Eur. Math. Soc.*, **8**:1–48, 2006.
- [18] F. MOKHTARIAN - S. ABBASI - J. KITTLER. Robust and efficient shape indexing through curvature scale space. *Proc. 6th British Machine Vision Conference*, pp 53–62, September 1996.
- [19] J. GLAUNES - A. TROUVE - L. YOUNES. Modeling planar shape variation via Hamiltonian flows of curves. *Model. Simul. Sci. Eng. Technol.*, 335–361, 2007.
- [20] D. SHANKS. *Solved and unsolved problems in number theory*. Chelsea Publishing Co., 1993, p. 143.
- [21] D. SHARVIT - J. CHAN - B. B. KIMIA. Symmetry-based indexing of image databases. In *Content-Based Access of Image and Video Libraries*, 1998.
- [22] K. SIDDIQI - B. KIMIA. A shock grammar for recognition. *Proceedings of the Conference on Computer Vision and Pattern Recognition*, 1996, p. 507–513.
- [23] L. YOUNES. Jacobi fields in groups of diffeomorphisms and applications. *Quart. Appl. Math.*, **65**:113–134, 2007.

---

Received 4 July 2008,  
and in revised form 10 November 2008.

Dept. of Mathematics  
California State University  
Channel Islands  
Camarillo, CA 93012  
k\_leonard@alumni.brown.edu

